A CURVED BOX BEAM ELEMENT CONSIDERING SHEAR LAG EFFECT AND ITS STATIC AND DYNAMIC APPLICATIONS

Wu Yaping

State Key Laboratory of Frozen Soil Engineering, Cold and Arid Regions Environmental and Engineering Research Institute, Chinese Academy of Sciences, Lanzhou 730000, People's Republic of China. E-mail: wypsw@263.net; and

Department of Civil Engineering, Lanzhou Railway University, Lanzhou 730070, People's Republic of China

Lai Yuanming and Zhu Yuanlin

State Key Laboratory of Frozen Soil Engineering, Cold and Arid Regions Environmental and Engineering Research Institute, Chinese Academy of Sciences, Lanzhou 730000, People's Republic of China

AND

Pan Weidong

Department of Geology, Lanzhou University, Lanzhou 730000, People's Republic of China

1. INTRODUCTION

Thin-walled curved beams with closed and open cross-sections are widely used in the construction of bridges. Although there are many methods (e.g., methods of finite-shell-element, finite-strip-element and folded-plate, etc.) to analyze these structures, for reasons that are well known, finite beam element method has many advantages in economy and analysis. For the analytical method of curved thin-walled beams, the general solution of the static problem was given by Vlasov [1] and Dabrowski [2]. Later, some researchers developed foregoing theories by adding shear lag effect and neglecting secondary warping shear effect caused by warping torsion in curved thin-walled beams [3–5]. As to finite element analysis, for the problem researchers have published many papers on the static and dynamic analysis of curved box beams [6–8] over the past decades, But summarily, the procedures utilizing curved beam element method and considering both shear lag and warping torsion effects, especially for the dynamical analysis of curved thin-walled multicell box beams, may still be lacking.

For the problem mentioned above, this paper presents a finite curved beam element method of analyzing the static and dynamic behaviors of curved thin-walled box beam bridge based on the energy principle. In the procedure, the shear lag, warping torsion and rotational inertia effects are taken into account to formulate the stiffness matrix and mass matrix. In the application example, free vibration characteristics and responses of the normal stress and vertical displacement to static load, moving load and earthquake load were analyzed, some meaningful results were obtained which can provide reference for structure designer.

2. STATIC BACKGROUND OF CURVED BOX BEAM ELEMENT

The layout of curved thin-walled multicell box beam element with corresponding circular cylindrical co-ordinate system is shown in Figure 1. The translation of cross-section in x, y, z directions is denoted as u, v, w respectively. The angular rotation of cross-section about x-, and y-axis and shear center are denoted as θ_x, θ_y, θ_z respectively. The warping function associated with the warping torsion and shear lag effects are denoted as β, ϕ respectively.

Assuming that shear lag-induced flange axial warping displacement along the flanges can be expressed by

$$W_s = \frac{R}{\rho} f(x, y)\phi = \frac{R}{\rho}[w_{s0} - yw_s]\phi(z), \tag{1}$$

where $f(x, y)$ is the shear lag-induced warping modality, $w_s(x)$ is the non-uniform distribution function along the flanges which can be expressed by a cubic parabola for signal cell or multicell box beams [9], w_{s0} = constant which is determined by $\int_A \sigma_s \, dA = 0$, ρ is the radius of curvature at any point.

Considering the influence of curvature, the shear lag-induced normal stress and shear stress can be obtained, respectively, by

$$\sigma_s = E\frac{\partial W_s}{\partial z} = E\frac{R}{\rho}[w_{s0} - yw_s(x)]\phi'(x), \tag{2}$$

$$\tau_s = G\frac{\partial W_s}{\partial x} = -G\frac{R}{\rho}\frac{dw_s}{dx}y\phi(z), \tag{3}$$

where "$'$" denotes (d/dz). Obviously, equation (3) satisfies the equilibrium condition $\int_A \tau_s \, dA = 0$.

The shear lag-induced vertical bending moment M_{sx} can be obtained by

$$M_{sx} = \int_A \sigma_s y \, dA = -EI_{sx}\phi', \tag{4}$$

where $I_{sx} = -\int_A (R/\rho)yf(x, y)\,dA$.

Considering equations (2) and (4), the total vertical bending moment and the corresponding normal stress can be obtained, respectively, by

$$M_x = -EI_x\left(v'' + \frac{\theta_z}{R^2}\right) - EI_{sx}\phi', \tag{5}$$

$$\sigma_b = \frac{R}{\rho}\left[-Ey\left(v'' + \frac{\theta_z}{R^2}\right) + E(w_{s0} - yw_s(x))\phi'\right] = \frac{R}{\rho}\left[\frac{M_x - M_{sx}}{I_x}y - (w_{s0} - yw_s)\frac{M_{sx}}{I_{sx}}\right]. \tag{6}$$
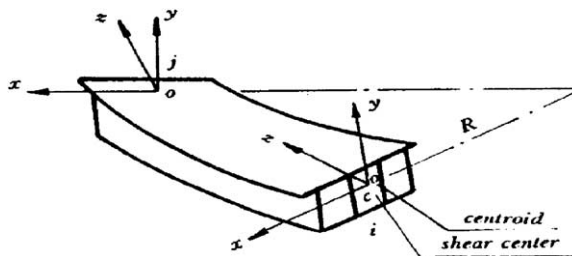

Figure 1. Curved box beam element.

The total normal stress is

$$\sigma_z = \frac{R}{\rho}\left[\frac{N}{A} + \frac{M_x - M_{sx}}{I_x}y - (w_{s0} - yw_s)\frac{M_{sx}}{I_{sx}} - \frac{M_y}{I_y}x + \frac{B}{I_{\hat{\omega}}}\hat{\omega}\right], \tag{7}$$

where N is the axial force, M_y is the lateral bending moment, B is the bi-moment, $\hat{\omega}$ is a fan-shaped co-ordinate (unitage of torsion warping deformation), M_x and M_{sx} are determined by M_{xB}, B and M_ϕ (see equations (11) and (12)).

Neglecting the strain energy due to the bending shear strain, the strain energy stored within the curved box beam element can be given by

$$U_1 = \frac{1}{2}\int_0^l \frac{N^2}{EA}\mathrm{d}z + \frac{1}{2}\int_0^l \frac{M_y^2}{EI_y}\mathrm{d}z + \frac{1}{2}\int_0^l \frac{T_{sv}^2}{GK_t}\mathrm{d}z + \frac{1}{2}\int_0^l \frac{T_{\hat{\omega}}^2}{G(K_t - I_c)}\mathrm{d}z + \frac{1}{2}\int_0^l \frac{B^2}{EI_{\hat{\omega}}}\mathrm{d}z$$
$$+ \frac{1}{2}\iint\left(\frac{\sigma_b^2}{E} + \frac{\tau_s^2}{G}\right)\mathrm{d}A\,\mathrm{d}z \tag{8}$$

in which, the fourth item is caused by secondary warping shear, T_{sv} is St Venant's torque, $T_{\hat{\omega}}$ is the warping torque.

The external loading-induced potential energy can be given by

$$U_2 = -\int_0^l (q_x u + q_y v + q_z w + m_z \theta_z)\,\mathrm{d}z$$
$$- (Q_x u + Q_y v + Nw + M_{xB}\theta_x + M_y\theta_y + B\beta + M_\phi\phi)|_0^l, \tag{9}$$

where Q is the shear force, q_x, q_y, and q_z are the distributed loads acting on the centroid of beam cross-section, m_z is the distributed torque about shear center, M_{XB} is the sum of vertical bending moment and coupling of bi-moment, M_ϕ is the internal force corresponding to ϕ.

The total potential energy can be given by

$$\Pi = U_1 + U_2. \tag{10}$$

Combining equations (8)–(10) via equations (3) and (6) and then, according to the principle of minimum potential energy $\delta\Pi = 0$, the internal forces corresponding to θ_x, ϕ are given as

$$M_{xB} = M_x + \frac{B}{R}, \qquad \delta\theta_x = -\delta v' \neq 0, \tag{11}$$

$$M_\phi = \left(\frac{I_{sx}}{I_x} - \frac{I_s}{I_{sx}}\right)M_{sx} - \frac{I_{sx}}{I_x}M_x, \qquad \delta\phi \neq 0. \tag{12}$$

For the beam element, we let $m_z = m_z' = 0$. Omitting the items of higher order, the bi-moment with consideration of shear lag effect can be expressed as

$$B = \frac{EI_{\hat{\omega}}}{\mu}\left[\beta' + \left(1 - 2\mu - \frac{EI_x}{GI_c}\right)\frac{v''}{R} - \frac{EI_{sx}}{GI_c}\frac{\phi}{R}\right], \tag{13}$$

where I_c is the central moment of inertia, K_t is St Venant's torsional constant, $\mu = 1 - K_t/I_c$, $k = EI_{\hat{\omega}}/G\mu^2 I_c$.

3. DYNAMICAL EQUATIONS FOR CURVED BOX BEAM ELEMENT

For a beam element, neglecting the difference between centroid and shear center and effect of couplings, based on the theory of dynamics, the kinetic energy of beam element due

to velocity vector and angular velocity vector can be expressed as

$$T = \frac{1}{2}\int_0^l \gamma A[(\dot{u})^2 + (\dot{v})^2 + (\dot{w})^2]\,\mathrm{d}z + \frac{1}{2}\gamma I_x \int_0^l (\dot{\theta}_x)^2\,\mathrm{d}z + \frac{1}{2}\gamma I_y \int_0^l (\dot{\theta}_y)^2\,\mathrm{d}z$$

$$+ \frac{1}{2}\gamma I_c \int_0^l (\dot{\theta}_z)^2\,\mathrm{d}z + \frac{1}{2}\gamma I_{\dot{\omega}} \int_0^l (\dot{\beta})^2\,\mathrm{d}z + \frac{1}{2}\gamma I_s \int_0^l (\dot{\phi})^2\,\mathrm{d}z \tag{14}$$

in which the fifth and sixth items are caused, respectively, by torsional warping effect and shear lag effect, γ denotes the mass density, " $\cdot$ " denotes (d/dt).

Utilizing polynomial as interpolation functions, the internal displacement vector of an element is given as

$$\eta = [N_\eta]\{\delta_\eta\} \quad (\eta = u, v, w, \varphi, \phi), \tag{15}$$

where $[N_\eta]$ denotes the shape function matrix, $\{\delta_u\} = [u_i \ \theta_{yi} \ u_j \ \theta_{yj}]^\mathrm{T}$, $\{\delta_v\} = [v_i \ \theta_{xi} \ v_j \ \theta_{xj}]^\mathrm{T}$, $\{\delta_\varphi\} = [\theta_{zi} \ \beta_i \ \theta_{zj} \ \beta_j]^\mathrm{T}$, $\{\delta_\phi\} = [\phi_i \ \phi_j]^\mathrm{T}$, $\{\delta_W\} = [w_i \ w_j]^\mathrm{T}$.

The equivalent nodal loading vector corresponding to η can be expressed as

$$\{R_\eta\} = \int_0^l [N_\eta]^\mathrm{T} p_\eta\,\mathrm{d}z \quad (\eta = u, v, w, \phi \text{ and } p_\eta = q_x, q_y, q_z, m_z). \tag{16}$$

Substitute equation (15) into equations (8), (9) and (16), respectively, and convert boundary forces in equation (9) into nodal force. Then, according to the Lagrange equations, the dynamic equations of curved beam element can be determined by

$$\frac{\mathrm{d}}{\mathrm{d}t}\left(\frac{\partial T_{12}}{\partial\{\dot{\delta}_\eta\}}\right) - \frac{\partial T_{12}}{\partial\{\delta_\eta\}} + \frac{\partial \Pi}{\partial\{\delta_\eta\}} = -[C_\eta]\{\dot{\delta}_\eta\} \quad (\eta = u, v, w, \varphi, \phi), \tag{17}$$

where $[C_\eta]$ is the damping matrix corresponding to η. Equation (17) can be expressed as

$$[M]^e\{\ddot{\delta}\}^e + [C]^e\{\dot{\delta}\}^e + [K]^e\{\delta\}^e = \{F\}^e + \{R\}^e, \tag{18}$$

where $[K]^e$ is the element stiffness matrix, $[M]^e$ is the element mass matrix, $[C]^e$ is the element damping matrix, $\{\delta\}^e$ is the element nodal displacement vector, $\{F\}^e$ is the element nodal loading vector, $\{R\}^e$ is the element equivalent nodal loading vector. For convenience, the above vectors can be arranged in the following order:

$$\{\delta\}^e = [u_i \ v_i \ w_i \ \theta_{xi} \ \theta_{yi} \ \theta_{zi} \ \beta_i \ \phi_i \ u_j \ v_j \ w_j \ \theta_{xj} \ \theta_{yj} \ \theta_{zj} \ \beta_j \ \phi_j]^\mathrm{T}, \tag{19}$$

$$\{F\}^e = [Q_{xi} \ Q_{yi} \ N_i \ M_{xBi} \ M_{yi} \ T_i \ B_i \ M_{\phi i} \ Q_{xj} \ Q_{yj} \ N_j \ M_{xBj} \ M_{yj} \ T_j \ B_j \ M_{\phi j}]^\mathrm{T}, \tag{20}$$

$$\{R\}^e = [R_1 \ R_2 \ R_3 \ R_4 \ R_5 \ R_6 \ R_7 \ 0 R_9 \ R_{10} \ R_{11} \ R_{12} \ R_{13} \ R_{14} \ R_{15} \ 0]^\mathrm{T}. \tag{21}$$

By element combination the dynamic responses of a carved bridge to moving load or seismic stimulation are determined by the following equation:

$$[M]\{\ddot{\delta}\} + [C]\{\dot{\delta}\} + [K]\{\delta\} = \{F\}, \tag{22}$$

where $[M]$, $[C]$, and $[K]$ are the global mass, global damping, and global stiffness matrix, respectively, $\{\delta\}$ and $\{F\}$ are the global nodal displacement and the global nodal loading vector respectively. In this paper, damping is assumed to be Rayleigh damping .

The generalized eigenvalue problem of free vibration equations of structure without damping is obtained by

$$[K]\{\Phi\} = \omega^2[M]\{\Phi\}, \tag{23}$$

where ω^2 is the eigenvalue, $\{\Phi\}$ is the eigenvector.

For a moving concentrated loading vector $\{P\}^e = [P_x \, P_y \, P_z \, M_z]^T$, the element distributed loading vector is

$$\{q\}^e = [q_x \quad q_y \quad q_z \quad m_x]^T = \{P\}^e\delta(z - vt), \tag{24}$$

where δ is the delta function, z is the position co-ordinate of moving loading, v is the velocity of moving loading vector.

By substituting equation (24) into the general calculating formula of equivalent nodal loads equation (16), the element equivalent nodal loading vector $\{R\}^e$ can be obtained, and then, by co-ordinate transformation and elements combination, global nodal vector $\{F\}$ can be determined.

For the seismic response analysis of the curved box beam bridge, vector $\{F\}$ is given by

$$\{F\} = -[M]\{\ddot{\delta}\}_g, \tag{25}$$

where $\{\ddot{\delta}\}_g$ is the earthquake acceleration.

4. APPLICATION EXAMPLES

Example 1. The layout of a two-cell curved continuous box beam with two equal spans is shown in Figure 2, the values used for elastic modulus, shear modulus, and mass density are $E = 3.28$ Gpa; $G = 1.26$ Gpa; and $\gamma = 2915.25$ kg/m^3. The curve length of every span and the wall thickness are $l/2 = 91.6$ cm, and $t = 0.5$ cm.

When a concentrated load $P_y = 200$ N acts on the inner web (point D) and moves with a speed of 0·229 m/s along the longitudinal direction of the curved beam, the responses of normal stresses at point F and vertical displacements at centroid on b–b section of this girder are calculated by using the present approach with eight equal curved beam elements. The numerical results of normal stress at point F (where the maximal stress occurs) on the section b–b are depicted in Figures 3 and 4 from which we can see that dynamic normal stress is 27·3% larger than the static normal stress, so when a curved box girder is subjected to a moving load, the impact effects of moving load on girder should be considered.

For the validation of the present approach, the structural analysis program SAPIV [10] was used here too with structure been divided by 120 shell elements. When a concentrated
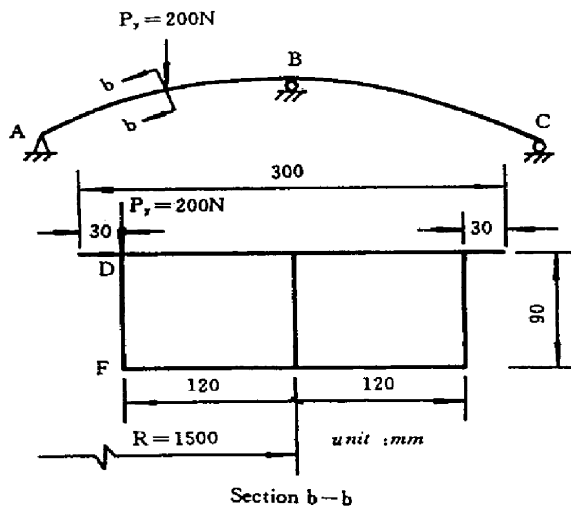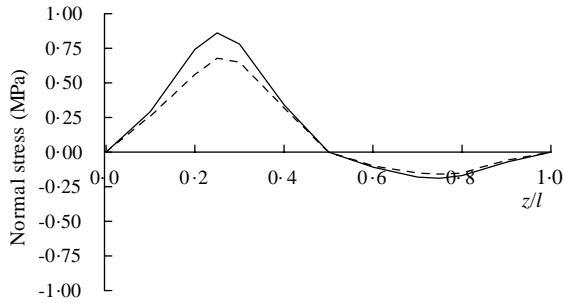

Figure 2. Example 1 and its cross-section.

Figure 3. Influence line of normal stress at point F on section b–b of Example 1. ——, Dynamic; – – – – –, Static.
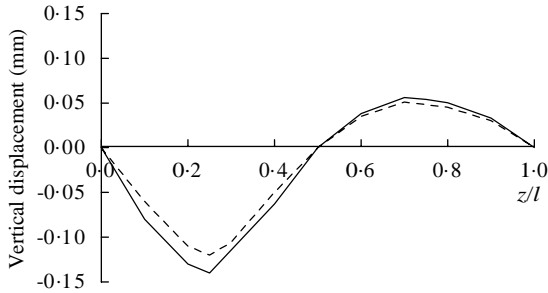

Figure 4. Influence line of vertical displacement at centroid on section b–b of Example 1. ——, Dynamic; – – – – –, Static.

TABLE 1

Comparison of normal stress at point F on section b–b of Example 1 *among various results* (MPa)

Present curved box beam element					
Bending induced value	Warping torsion induced value	Shear lag induced value	Total value	Shell element (SAPIV)	Model test
0·27	0·378	0·03	0·678	0·643	0·658

load P acts on section b–b (mid-span), for normal stress results at point F of section b–b its comparison among various procedures and its inscape are shown in Table 1, which shows that numerical results obtained by the present approach, SAPIV program, and model test are in good agreement.

Table 2 presents the first five natural frequencies of the beam calculated by using the present approach (with and without consideration of shear lag and warping torsion effects) and SAPIV program respectively. The data show that the results of the present approach with consideration of shear lag and warping torsion effects, especially for higher mode frequency, are closer to the results obtained from the shell element method of SAPIV program than those of the one without considering shear lag and warping torsion effects.

The seismic responses of normal stresses at point F and vertical displacements at centroid on b–b section of the structure to EL center wave (acceleration peak value is assumed to be

TABLE 2

The first five natural frequencies of Example 1 (Hz)

| Mode no. | Results of present curved box beam element | | Results of shell element (SAPIV) |
	Without shear lag and warping torsion effects	With shear lag and warping torsion effects	
1	76·13	81·58	78·76
2	114·89	109·86	105·58
3	117·70	116·95	111·88
4	182·46	153·83	145·81
5	220·40	175·64	164·76
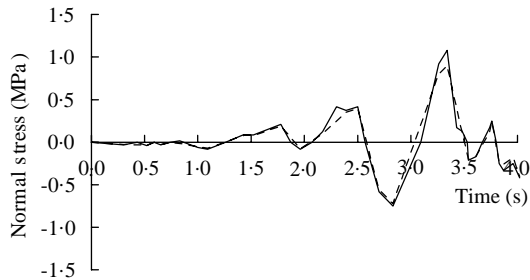
Figure 5. The seismic response of normal stress at point F on section b–b of Example 1. ——, Present; – – – –, SAPIV.
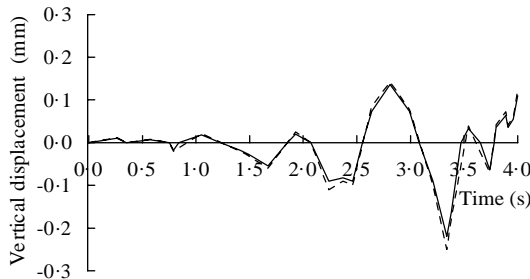

Figure 6. The seismic response of vertical displacement at centroid on section b–b of Example 1. ——, Present; – – – – –, SAPIV.

$0·2\,g$) in the first 4 s are shown, respectively, in Figures 5 and 6 from which we can see that the difference between results of the present procedure and results of SAPIV is small and both maximum values of normal stress and vertical displacement occur at time = 3·3 s.

Example 2. A cantilever curved single-cell box beam subjected to a concentrated load P at the tip is shown in Figures 7 and 8. Some of its geometry and material properties are given as: $E = 30\,000$ ksi, $G = 11\,600$ ksi, $\gamma = 5·555 \times 10^{-7}$ kip/in^3, radius of curvature $R = 2291·88$ in, curve length $l = 100$ ft.

Table 3 shows the convergence of vertical deflection with ξ, the number of curved beam elements, and closed-form solution of vertical displacements obtained by Dabrowski [2]. Table 4 shows the convergence of the first five natural frequencies with ξ. The data show that for the case where vertical displacements at various sections x/l are calculated, the limit
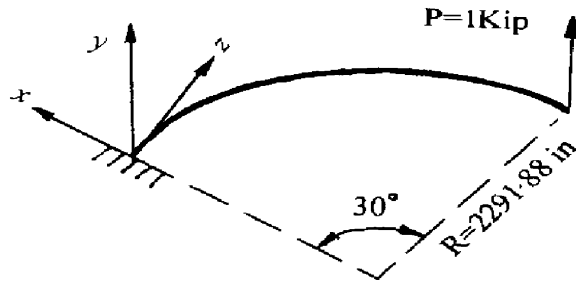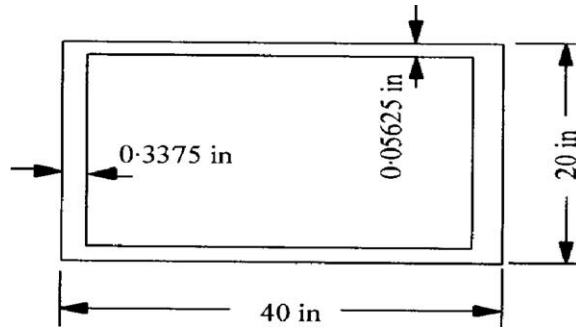
Figure 7. Sketch of Example 2.

Figure 8. Cross-section of the beam in Example 2.

TABLE 3

Convergence of vertical deflection and its comparison with closed-form solution for Example 2 (ft)

Cross-section z/l	Present results with ξ			Closed-form solution Dabrowski [2]
	5	10	15	
0	0·000	0·000	0·000	0·000
0·2	0·098	0·098	0·098	0·097
0·4	0·371	0·371	0·371	0·367
0·6	0·777	0·777	0·777	0·769
0·8	1·273	1·273	1·273	1·260
1·0	1·812	1·812	1·812	1·792

of convergence can be reached by $\xi = 5$ and due to the consideration of shear lag, the values of convergence of the present approach loosely-fit the closed-form solution (without considering shear lag), for the case where natural frequencies are calculated, the limit of convergence can be reached by $\xi = 5$ for lower mode frequencies and decreases with increasing ξ for higher mode frequencies, but convergent tendency is a stationary process.

5. CONCLUSIONS

The curved box beam finite element method presented by this paper has considered both shear lag and warping torsion (including secondary warping shear) effects and contribution

Table 4

Convergence of the first five natural frequencies of Example 2 (Hz)

Mode no.	Present results with ξ			
	5	10	15	20
1	0·6436	0·6436	0·6436	0·6436
2	1·5689	1·5688	1·5688	1·5688
3	3·8665	3·8612	3·8609	3·8609
4	9·9081	9·8943	9·8935	9·8934
5	11·088	10·977	10·971	10·970

of rotational inertia to mass matrix, so it can be used to analyze accurately the static and dynamic behaviors of curved thin-walled box bridge with single cell or multi-cell. Compared with the proceeding of finite shell element, the present approach is more concise and easy to use for the engineering designer. In the application examples, the numerical results obtained by the present approach show fair agreement with those obtained by model test or finite shell element method and convergence of elements presented by this paper is good.

ACKNOWLEDGMENTS

REFERENCES

1. V. Z. VLASOV 1961 *Thin-Walled Elastic Beams*. Washington, DC: National Science Foundation; second edition.
2. R. DABROWSKI 1968 *Curved Thin-Walled Girders*. London: Cement and Concrete Association.
3. H. KAORU, U. SEIZO and H. YASUSHI 1985 *Journal of Engineering Mechanics, American Society of Civil Engineers*, **111**, 87–92. Shear lag analysis and effective width of curved girder bridges.
4. K. K. KOO and Y. K. CHEUNG 1989 *Journal of Engineering Mechanics, American Society of Civil Engineers*, **115**, 2271–2286. Mixed variational formulation for thin-walled beams with shear lag.
5. Q. Z. LUO and Q. S. LI 2000 *Journal of Engineering Mechanics, American Society of Civil Engineers*, **126**, 1111–1114. Shear lag of thin-walled curved box girder bridges.
6. R. O. RABIZADEH 1974 PhD Dissertation, University of Pennsylvania, Philadelphia, PA. Static and dynamic analysis of horizontally curved box girder bridges.
7. F. B. HE 1981 *Journal of China Solid Mechanics* **2**, 141–157. The finite element method for thin-walled elastic curved beams.
8. C. C. FU and Y. T. HSU 1995 *Computers and Structures* **54**, 147–159. The development of an improved curvilinear thin-walled Vlasov lement.
9. Y. P. WU 1992 *Journal of Lanzhou Railway Institute* (China), **11**, 36–48. Analysis of shear lag in multicell box girder by means of variational calculus.
10. K. J. BATHE, E. L. WILSON and F. E. PETERSON 1973 *Report EERC* 73-11. College of Engineering, University of California, Berkeley, CA, June. SAPIV—a structural analysis program for static and dynamic response of linear systems.